

Article

# Effect of the $\text{SiCl}_4$ Flow Rate on SiBN Deposition Kinetics in $\text{SiCl}_4\text{-BCl}_3\text{-NH}_3\text{-H}_2\text{-Ar}$ Environment

Jianping Li, Hailong Qin, Yongsheng Liu \*, Fang Ye, Zan Li, Laifei Cheng and Litong Zhang

Science and Technology on Thermostructural Composite Materials Laboratory, Northwestern Polytechnical University, Xi'an 710072, Shaanxi, China; [ijianping@163.com](mailto:ijianping@163.com) (J.L.); [qinxlong555@163.com](mailto:qinxlong555@163.com) (H.Q.); [yefang511@nwpu.edu.cn](mailto:yefang511@nwpu.edu.cn) (F.Y.); [zli4\\_07@163.com](mailto:zli4_07@163.com) (Z.L.); [chenglf@nwpu.edu.cn](mailto:chenglf@nwpu.edu.cn) (L.C.); [zhanglt@nwpu.edu.cn](mailto:zhanglt@nwpu.edu.cn) (L.Z.)

\* Correspondence: [yongshengliu@nwpu.edu.cn](mailto:yongshengliu@nwpu.edu.cn) or [liuys99067@163.com](mailto:liuys99067@163.com); Tel.: +86-29-8849-5179; Fax: +86-29-8849-4620

Academic Editor: Christof Schneider

Received: 29 March 2017; Accepted: 31 May 2017; Published: 7 June 2017

**Abstract:** To improve the thermal and mechanical stability of  $\text{SiC}_f/\text{SiC}$  or  $\text{C}/\text{SiC}$  composites with SiBN interphase, SiBN coating was deposited by low pressure chemical vapor deposition (LPCVD) using  $\text{SiCl}_4\text{-BCl}_3\text{-NH}_3\text{-H}_2\text{-Ar}$  gas system. The effect of the  $\text{SiCl}_4$  flow rate on deposition kinetics was investigated. Results show that deposition rate increases at first and then decreases with the increase of the  $\text{SiCl}_4$  flow rate. The surface of the coating is a uniform cauliflower-like structure at the  $\text{SiCl}_4$  flow rate of 10 mL/min and 20 mL/min. The surface is covered with small spherical particles when the flow rate is 30 mL/min. The coatings deposited at various  $\text{SiCl}_4$  flow rates are all X-ray amorphous and contain Si, B, N, and O elements. The main bonding states are B-N, Si-N, and N-O. B element and B-N bonding decrease with the increase of  $\text{SiCl}_4$  flow rate, while Si element and Si-N bonding increase. The main deposition mechanism refers to two parallel reactions of  $\text{BCl}_3+\text{NH}_3$  and  $\text{SiCl}_4+\text{NH}_3$ . The deposition process is mainly controlled by the reaction of  $\text{BCl}_3+\text{NH}_3$ .

**Keywords:** SiBN coating; low pressure chemical vapor deposition;  $\text{SiCl}_4$  flow; deposition mechanism

## 1. Introduction

Continuous fiber reinforced silicon carbide ceramic matrix composite (CFCC-SiC) are considered as one of the most promising new generation of thermo-structural materials, which exhibit excellent properties in many aspects, such as high temperature resistance, low density, high specific strength, high specific modulus, antioxidant ablation, and high reliability [1,2]. Interphase is the key microstructure unit for strengthening-toughening of CFCC-SiC and h-BN is widely used as the interphase of  $\text{SiC}/\text{SiC}$  composites [3–5]. However, the oxidation resistance of BN interphase is still poor when  $\text{SiC}_f/\text{SiC}$  or  $\text{C}_f/\text{SiC}$  composites are used at relatively higher temperatures and in an oxidizing environment. The oxidizing medium could spread to fibers, leading to the oxidation of composites and failure to meet the application requirement under the high temperature oxidizing environment for a long time [4]. Consequently, it is necessary to improve the oxidation resistance of the BN interphase in  $\text{SiC}_f/\text{BN}/\text{SiC}$  and  $\text{C}_f/\text{SiC}$  composite.

Silicon is one of the high temperature stable elements. What's more, oxygen diffuses more slowly in  $\text{SiO}_2$  glass than that in  $\text{B}_2\text{O}_3$  glass [6]. In recent study of  $\text{SiC}_f/\text{BN}/\text{SiC}$  composite, BN coating will be oxidized and gasified in 1–10%  $\text{P}_{\text{H}_2\text{O}}$  environment at 700–800 °C, even though the h-BN was deposited at 1800 °C. The BN coatings deposited at 1060 °C and 1400 °C are even worse. However, the BN interphase containing 22 wt % Si element deposited at 1400 °C survived after work for 1000 h in the same environment [7]. Therefore, doping BN interphase with Si will be an effective way to improve the antioxidant ability of the BN interphase in  $\text{SiC}_f/\text{BN}/\text{SiC}$  composites or  $\text{C}_f/\text{BN}/\text{SiC}$  composites.

Much work has been done in the study of SiBN coating. Moore et al. [8] deposited SiBN interphase at 1400 °C using BCl<sub>3</sub>-NH<sub>3</sub>-SiHCl<sub>3</sub>-H<sub>2</sub>-N<sub>2</sub>-Ar mixture via chemical vapor deposition (CVD). Thanks to the doping of 15–40 wt % Si element, the SiBN interphase enhanced the oxidation resistance of composites 2–3 times more than pure BN at 1200–1500 °C and was more resistant to the reaction with moisture. Nakamura et al. [9] deposited SiBN coating using (C<sub>2</sub>H<sub>5</sub>)<sub>3</sub>SiH (TES)-(C<sub>2</sub>H<sub>5</sub>)<sub>3</sub>B (TDB)-NH<sub>3</sub> mixture via metalorganic chemical vapor deposition (MOCVD). The coating was amorphous. Results showed that the temperature and the flow ratio of TES and TDB influence the deposition process a lot. Essafti et al. [10] deposited SiBN coating at 800 °C using B<sub>2</sub>H<sub>6</sub>-NH<sub>3</sub>-SiH<sub>4</sub>-H<sub>2</sub> mixture via CVD. SiBN coating was deposited through two parallel reactions of B<sub>2</sub>H<sub>6</sub>+NH<sub>3</sub> and SiH<sub>4</sub>+NH<sub>3</sub> and the flow ratio SiH<sub>4</sub>/B<sub>2</sub>H<sub>6</sub> determines the micro components of the coating. The amorphous SiBN can be deposited using SiCl<sub>4</sub>-BCl<sub>3</sub>-NH<sub>3</sub>-H<sub>2</sub>-Ar mixture. The effect of temperature on SiBN deposition and the relationship between SiBN interphase and composites' mechanical properties have been discussed in our previous work [11–14]. So far, the flow of reactants, an important factor influencing the deposition, has been rarely reported.

In this paper, the SiBN coating was deposited on carbon cloth systematically using SiCl<sub>4</sub>-BCl<sub>3</sub>-NH<sub>3</sub>-H<sub>2</sub>-Ar as the reaction mixture at 900 °C under a SiCl<sub>4</sub> flow rate ranging from 10 mL/min to 30 mL/min. The effect of SiCl<sub>4</sub> flow rate on the deposition kinetics—including deposition rate, morphology, phase composition, chemical composition, and bonding states of SiBN coating—was investigated. Additionally, the deposition mechanism was discussed.

## 2. Materials and Methods

### 2.1. Materials and Preparation Method

In the CVD gas system of SiCl<sub>4</sub>-BCl<sub>3</sub>-NH<sub>3</sub>-H<sub>2</sub>-Ar, SiCl<sub>4</sub> (purity 99.99 wt %) was used as silicon resource; BCl<sub>3</sub> (purity 99.9 wt %) was used as boron resource; NH<sub>3</sub> (purity 99.99 wt %) was used as nitrogen resource; H<sub>2</sub> (purity 99.999 wt %) was the dilution gas and carrier gas which delivered SiCl<sub>4</sub> from the bubbler to the reactor; and Ar (purity 99.999 wt %) was the protection gas. Carbon cloth woven with T300 carbon fiber (Toray Co., Tokyo, Japan) was used as deposition substrate.

The SiCl<sub>4</sub> reactant was carried into the reactor by H<sub>2</sub> via bubbling and the amount of SiCl<sub>4</sub> delivered by H<sub>2</sub> could be calculated by the formula

$$F_T = \frac{2.24 \times 10^{-2} P_T F_C}{RT} \quad (1)$$

where  $F_T$  is the flow rate (mL/min) of SiCl<sub>4</sub> carried by H<sub>2</sub>;  $P_T$  is the saturated vapor pressure (Pa) of SiCl<sub>4</sub> at certain temperature  $T$ ;  $F_C$  is the flow rate (mL/min) of carrier H<sub>2</sub>;  $R$  is the gas constant (8.314 J/(mol K));  $T$  is the temperature (K) of SiCl<sub>4</sub> liquid. In this work,  $T$  is set at 30 °C and  $P_T = 38.738$  kPa, according to NIST Chemistry WebBook search.

Hot-wall CVD reactor was used for SiBN coating deposition, and the deposition parameters are shown in Table 1. Before depositing the SiBN coating, carbon cloths, bunched with carbon fiber, were suspended in the reactor and the reactor was evacuated to the desired pressure and heated up to the deposition temperature. Then the reactants were introduced into the reactor, starting the deposition. After the deposition, reactants and power were cut off. The reactor was filled with argon to the atmospheric pressure when it was cooled down to room temperature. Then samples were removed from the reactor for analysis.

**Table 1.** Deposition parameters of SiBN coating with SiCl<sub>4</sub>-BCl<sub>3</sub>-NH<sub>3</sub>-H<sub>2</sub>-Ar system via low pressure chemical vapor deposition (LPCVD)

Substrate	T (°C)	T (h)	Q <sub>SiCl4</sub> (mL/min)	Q <sub>BCl3</sub> (mL/min)	Q <sub>NH3</sub> (mL/min)	Q <sub>H2</sub> (Dilution) (mL/min)	Q <sub>Ar</sub> (mL/min)	P (kPa)
Carbon cloth	900	7	102030	20	60	100	100	1

## 2.2. Characterization Method

The surface and cross-section morphologies of T300 carbon cloth after CVD SiBN coating were observed with scanning electron microscopy (SEM, S-2700, Hitachi, Tokyo, Japan). In order to get the deposition rate, 10 different positions distributed on different fibers uniformly around the cross-sectional edge were observed. The deposition rate was calculated via the equations

$$\bar{H} = \frac{H_1 + H_2 + \dots + H_{10}}{10} \quad (2)$$

$$v = \frac{\bar{H}}{t} \quad (3)$$

where the  $\bar{H}$  refers to the average thickness (nm) of SiBN coating;  $H_i$  ( $i = 1, 2, \dots, 10$ ) refers to the thickness (nm) of SiBN at different positions;  $v$  refers to the deposition rate (nm/h);  $t$  refers to the deposition time (h).

X-ray diffraction (XRD, X'Pert pro, Philip; Cu K-Alpha,  $\lambda = 0.154$  nm) was used to characterize the phase composition of the SiBN coating with a scanning speed of 0.1 s/step with  $0.02^\circ$ /step from  $10^\circ$  to  $90^\circ$ . The element types, element content and chemical bonding states of the SiBN coating were analyzed by X-ray photoelectron spectroscopy (XPS, Al K-Alpha, Thermo Scientific, New York, NY, USA) with pass energy of 100 eV, energy step of 1.0 eV, and number of energy steps is 1361.

## 3. Results and Discussion

### 3.1. Deposition Rate

The deposition rate of SiBN coating and average weight percent gain of samples at various flow rate of  $\text{SiCl}_4$  at  $900^\circ\text{C}$  are drawn in Figure 1. The results indicate that deposition rate varies greatly with the increase of  $\text{SiCl}_4$  flow rate. It increases at first and then decreases. The maximum deposition rate was obtained at about 20 mL/min. After 7 h of deposition the average thickness of SiBN ceramic film was about  $50 \mu\text{m}$  and the average weight percent gain of samples was 266%. The lowest one appears at the flow rate of 10 mL/min with the average deposition thickness of  $10 \mu\text{m}$  and the weight percent gain of 73%. The deposition rate at 30 mL/min is lower than that at 20 mL/min. It does not mean that the reaction rate decreases with the increase of reactant flow rate, but the increase of reaction rate promotes gas nucleation, thus reducing the amount of reactant. This consequently reduces the amount of the material deposited on the substrate. This will be discussed further in Section 3.2.

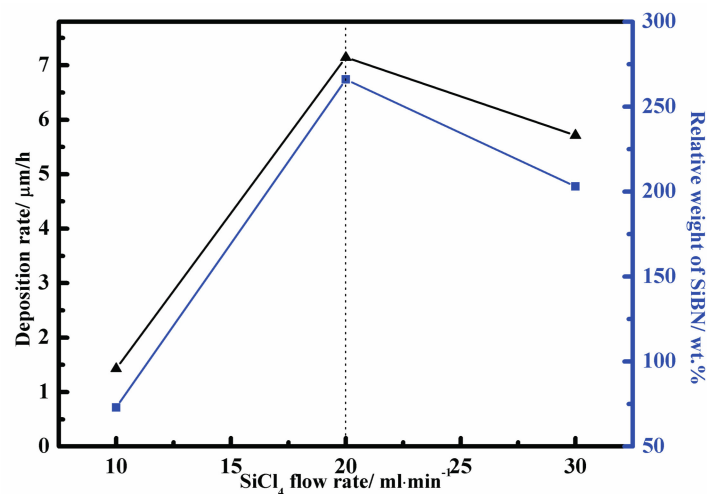


**Figure 1.** Deposition rate of SiBN coating and average weight percent gain of samples at various  $\text{SiCl}_4$  flow rate.

### 3.2. Morphology

The SEM images of the surface and cross-section of carbon cloth after CVD SiBN are presented in Figures 2 and 3. As shown in Figure 2, the surface morphologies of SiBN ceramic deposited at various SiCl<sub>4</sub> flow rates are different from each other. SiBN coating, deposited at the flow rate of 10 mL/min, was a uniform cauliflower-like structure, dense and smooth. When SiCl<sub>4</sub> flow rate is 20 mL/min, the cauliflower-like structure is bigger than that deposited at 10 mL/min. Besides, there are many small spherical particles closely packed on the surface, which make the surface rough. As the SiCl<sub>4</sub> flow rate rises to 30 mL/min, the SiBN cauliflower-like structure reduces and smaller spherical particles appear on the rough surface.

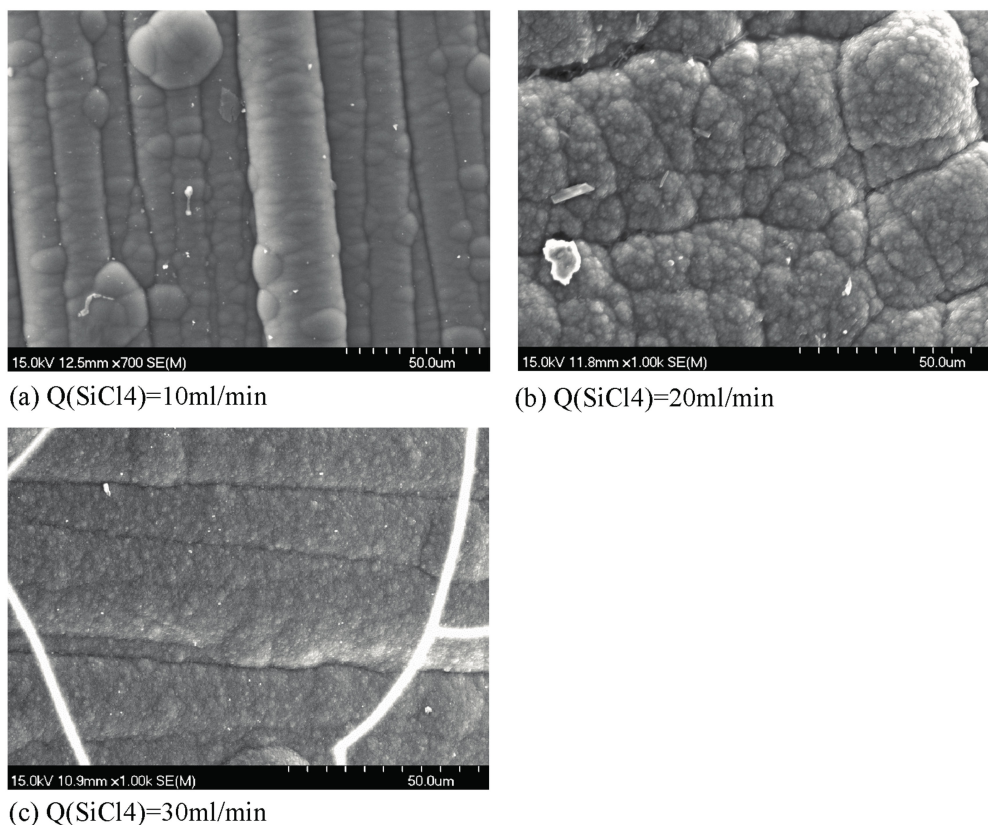


**Figure 2.** Scanning Electron Microscopy (SEM) images of surface morphologies of SiBN ceramic deposited at various SiCl<sub>4</sub> flow rates (a) Q(SiCl<sub>4</sub>) = 10 mL/min; (b) Q(SiCl<sub>4</sub>) = 20 mL/min; (c) Q(SiCl<sub>4</sub>) = 30 mL/min.

Based on the CVD theory, liquid drops of SiBN are initially formed on the substrate which solidify to form the SiBN film. One droplet grows to a bubble of cauliflower-like structure. The chemical reaction rate in CVD process increases with the concentration of reactants. With the increase of SiCl<sub>4</sub> flow rate, increased sizes of SiBN droplets are formed on the substrate, creating bigger cauliflower-like structure. When the droplets are big enough, they will spread and contact to each other, forming a flat structure and then causing the decrease of cauliflower-like structure. When the chemical reaction reaches a certain level, small spherical particles are nucleated in gas phase, which adhere on the surface of the sample by physical or chemical adsorption. This phenomenon, so-called gas-phase nucleation [15], can result in great fall of deposition rate for it consumes many reactants. To explain the influence of SiCl<sub>4</sub> flow rate on gas-phase nucleation, the equations below are needed.

$$r_c = \frac{2\sigma V_m}{RT\gamma} \quad (4)$$

$$J = (4\pi r_c^2) \cdot \alpha_c P (2\pi m RT)^{-\frac{1}{2}} \cdot n_i \cdot \exp\left(-\frac{\Delta G_c}{RT}\right) \quad (5)$$

where  $r_c$  is the critical nucleation radius;  $\sigma$  is surface energy per unit area;  $V_m$  is the molecule volume of species at nucleation temperature;  $R$  is the mole gas constant ( $R = 8.314 \text{ J}/(\text{mol K})$ );  $\gamma$  is the degree of super saturation;  $J$  is the nuclei formation rate;  $\alpha_c$  is the condensation coefficient of nuclei;  $P$  is the vapor pressure of reactant;  $n_i$  is the concentration of nuclei;  $\alpha_c P (2\pi m RT)^{-1/2}$  is the kinetic frequency factor; and  $-\Delta G_c$  is the critical Gibbs energy of nuclei formation. According to Equations (4) and (5), the gas-phase nuclei formation rate increases with the rise of the vapor pressure of reactant which is proportional to the  $\text{SiCl}_4$  flow. Therefore, more nuclei are formed in the gas environment, creating small spherical particles.

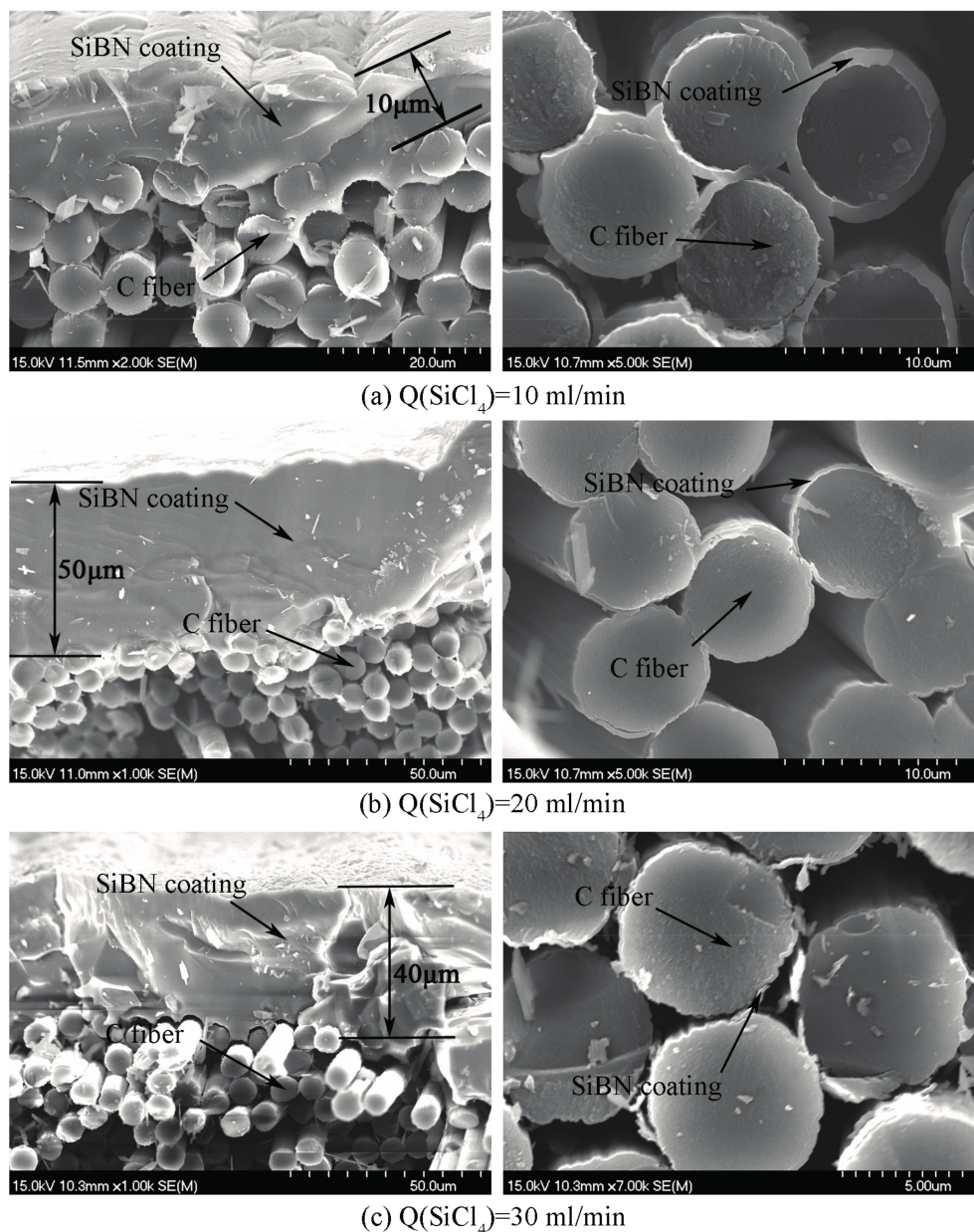


**Figure 3.** SEM images of cross-section morphologies of SiBN ceramic deposited at various  $\text{SiCl}_4$  flow rates (a)  $Q(\text{SiCl}_4) = 10 \text{ mL/min}$ ; (b)  $Q(\text{SiCl}_4) = 20 \text{ mL/min}$ ; (c)  $Q(\text{SiCl}_4) = 30 \text{ mL/min}$ .

The cross-sectional morphologies at various  $\text{SiCl}_4$  flow rates are showed in Figure 3. It is concluded that  $\text{SiCl}_4$  flow rate has a significant effect on the thickness of SiBN coating. When  $\text{SiCl}_4$  flow rate is 10 mL/min, the thickness of the SiBN coating on the surface of the carbon cloth (outer) is 10  $\mu\text{m}$  and the thickness of the coating surrounds (inner) the fibers is 1  $\mu\text{m}$ , which accounts for the comparatively low deposition rate. With the increase of  $\text{SiCl}_4$  flow rate, the deposition rate increases, leading to more SiBN deposited on the surface of the cloth and less deposited inside it. When the  $\text{SiCl}_4$  flow rate is 20 mL/min, the deposition thickness on the cloth is 50  $\mu\text{m}$  and inside the cloth is 200 nm. When the flow rate arrives 30 mL/min, the deposition thickness on the surface is 40  $\mu\text{m}$  and inside the cloth is about 200 nm.

The deposition rate increases with the increase of  $\text{SiCl}_4$  flow rate; thus, more SiBN ceramic will be deposited on the surface of carbon cloth. As the gas-phase nucleation occurs, the thickness of SiBN coating on the surface decreases due to the consumption of reactants in the gas environment. On the contrary, increased deposition rate leads to thinner SiBN coating deposited inside the carbon cloth. The thickness gradient of SiBN coating inside and outside increases as well. Infiltration depth and uniformity mainly depend on the deposition rate and the diffusion in carbon cloth, and the deposition rate plays a more important role at high temperature. The effective diffusion coefficient ( $D_{\text{eff}}$ ) is based on the Fick diffusion coefficient ( $D_F$ ) and the Knudsen diffusion coefficient ( $D_K$ ) with the Equation (6).

$$\frac{1}{D_{\text{eff}}} = \frac{1}{D_F} + \frac{1}{D_K} \quad (6)$$

At the beginning of deposition, the pore diameter is big enough to allow the reactant molecules diffuse into the carbon cloth by Fick diffusion. The diffusion is mainly related to temperature and pressure as Equation (7) shows.

$$D_F = D_0 T^m P^{-1} \quad (7)$$

where  $D_0$  refers to a constant;  $T$  refers to temperature (K);  $P$  refers to pressure (Pa);  $1.5 < m < 2$ . During this time, the deposition inside the cloth is mainly determined by the reaction. As more material is deposited on the surface, the pores which allow gas molecules to enter the cloth become smaller. When the pore diameter is comparable to or smaller than the mean free path of the diffusing reactant molecules, the Knudsen diffusion occurs.

$$D_K = \frac{d_p}{3} \left( \frac{8RT}{M} \right)^{3/2} \quad (8)$$

where  $d_p$  refers to the pore diameter;  $T$  refers to the temperature;  $M$  refers to the amount of reactants;  $R$  refers to mole gas constant ( $R = 8.314 \text{ J}/(\text{mol K})$ ). Equation (8) shows that Knudsen diffusion is relevant to the type of reactant, temperature, and pore diameter, but has nothing to do with the pressure which is a big difference from Fick diffusion. The gas molecules collide with the pore walls more frequently than with each other, so that it is hard to diffuse. During this time, the deposition inside the cloth is mainly determined by the diffusion. The more  $\text{SiCl}_4$  is consumed in the deposition, the quicker the deposition reaches the second stage. It is the reason that the thickness of SiBN coating inside the carbon cloth deposited at 20 mL/min is much thinner than that at 10 mL/min. With the continuous increase of  $\text{SiCl}_4$  flow rate, the thickness on the edge levels off. For the internal pores within carbon cloth, thickness of coatings on the internal fibers is independent with the reactant content and is related to temperature and the pore size, according to Equation (7). Thus, before the closure of the pore channel on the edge occurred, the diffusion and deposition on the internal fibers almost did not change when  $\text{SiCl}_4$  flow rate increased from 20 mL/min to 30 mL/min.

### 3.3. Phase Composition, Chemical Composition, and Bonding States

The composition and crystallinity of the SiBN coating deposited at various  $\text{SiCl}_4$  flow rates are examined by X-ray powder diffraction (XRD), as shown in Figure 4. There are no BN and  $\text{Si}_3\text{N}_4$

diffraction peaks, and the strong graphite peaks at  $26.603^\circ$  and  $44.666^\circ$  come from the substrate of carbon cloth. It indicates that the deposition products are X-ray amorphous, which is consistent with the result analyzed with transmission electron microscopy (TEM) in our previous work [14]. The peaks of graphite at 10 mL/min are much stronger than those at 20 mL/min and 30 mL/min, especially the peak at  $26.603^\circ$ . It is because that the thickness of SiBN coating grows with the increase of  $\text{SiCl}_4$  flow rate.

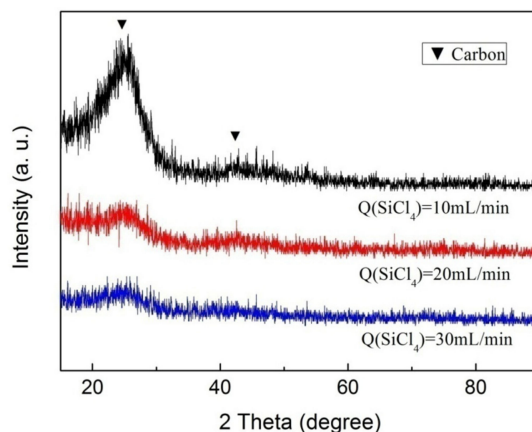


**Figure 4.** X-ray powder diffraction (XRD) patterns of SiBN ceramic deposited at various  $\text{SiCl}_4$  flow rates.

To determine the element types, element contents, and chemical bonding states of the SiBN coating, XPS analysis is carried out. Table 2 shows the elements and their contents in SiBN coating deposited at various  $\text{SiCl}_4$  flow rates. As can be seen, Si, B, N, and O are observed in all the products. B content decreases with the increase of  $\text{SiCl}_4$  flow rate, while Si content increases and O content remains relatively steady in the vicinity of 14–17 at.%.

**Table 2.** Element content of SiBN ceramic deposited at various  $\text{SiCl}_4$  flow rates analyzed by X-ray photoelectron spectroscopy (XPS).

$\text{SiCl}_4$ Flow Rate (mL/min)	Element Content (at.%)			
	B	N	Si	O
10	42.10	36.88	6.33	14.69
20	31.09	38.73	14.30	15.88
30	30.38	33.82	18.81	16.98

XPS is such a kind of surface analysis technology whose test depth is generally ranged from a few to tens of nanometers. In order to protect the bonding on the surface from being damaged, the samples are not etched before the test. The active part, lowly crystalline BN, on the surface is easy to be oxidized while being exposed in the air. It is the reason why the content of O element is a bit high.

Characterization of the chemical bonding in the SiBN coating is done with XPS, which offers the composition and the bonding types of atoms. The XPS data is transformed into N1s spectra according to the relationship between the Si, B, N, and O element bonding states and bonding energy, as shown in Figure 5. It shows that the bonding types are the same at various  $\text{SiCl}_4$  flow rates. There are three main types of bonding in SiBN coating—namely Si-N, B-N, and N-O—which are consistent with our previous work about the effect of deposition temperature on the deposition [13]. However, the content of them varies at various  $\text{SiCl}_4$  flow rates, as shown in Table 3. With the increase of  $\text{SiCl}_4$  flow rate, the content of B-N bonding decreases, while that of Si-N bonding increases. As for N-O bonding, there is not obvious rule about it. This content goes up and down at various  $\text{SiCl}_4$  flow rates. This is because N-O bonding is formed due to the oxidation of the surface when samples are exposed in the air as discussed above.

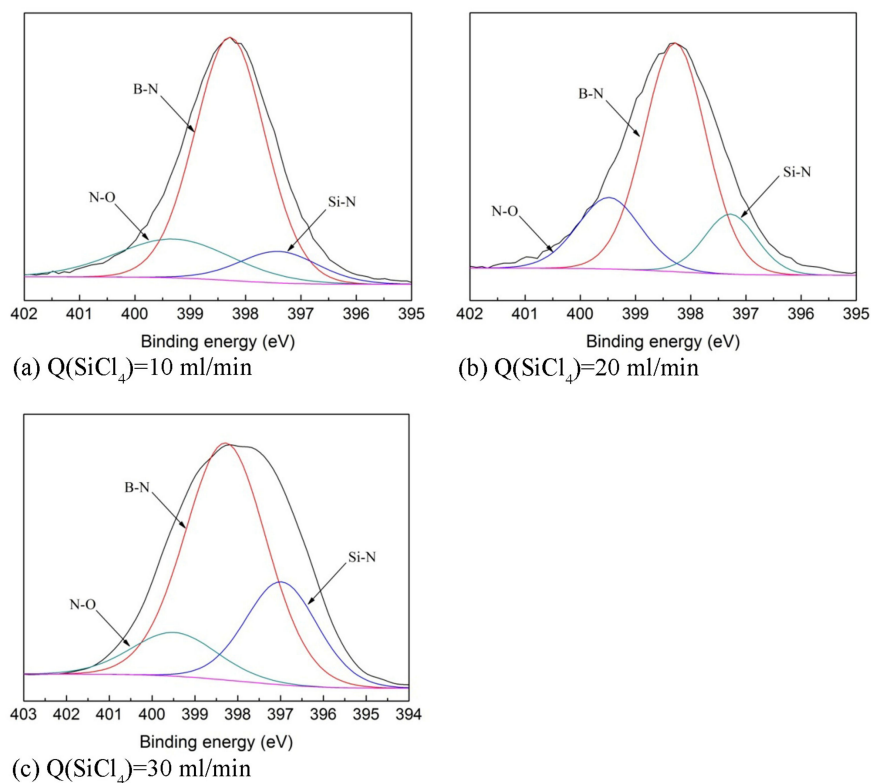


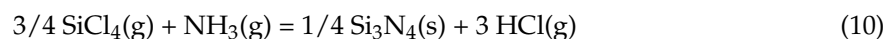
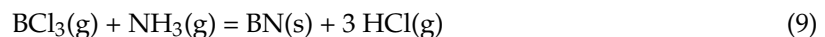
**Figure 5.** N1s spectra of SiBN ceramic deposited at various SiCl<sub>4</sub> flow rates (a) Q(SiCl<sub>4</sub>) = 10 mL/min; (b) Q(SiCl<sub>4</sub>) = 20 mL/min; (c) Q(SiCl<sub>4</sub>) = 30 mL/min.

**Table 3.** Bonding states of N1s and bonding content of SiBN coatings deposited at various SiCl<sub>4</sub> flow rates.

SiCl <sub>4</sub> Flow Rate (mL/min)	Bonding Content (at.%)		
	N-B (398.28 eV)	N-Si (397.40 eV)	N-O (399.28 eV)
10	71.11	10.27	18.62
20	65.01	14.34	20.65
30	63.45	24.25	12.30

### 3.4. Deposition Mechanism

The deposition rate, chemical composition, and bonding states are all determined by the deposition chemical reactions of the gas system. In the gas system of SiCl<sub>4</sub>-NH<sub>3</sub>-BCl<sub>3</sub>-H<sub>2</sub>-Ar, the main reaction equations are:



At 900 °C, reaction (9) is the dominant reaction because the Gibbs energy ( $\Delta G$ ) of Equation (9),  $-191.414$  KJ (calculated with Factsage software, Thermofact /CRCT and GTT-Technologies, Montreal, Canada and Herzogenrath, Germany) is much lower than that of reaction (10),  $-91.768$  KJ. Therefore, the content of B element is much higher than Si and the main bonding state of N element is B-N, as shown in Tables 2 and 3. The deposition of SiBN coating can be regarded as the co-deposition of X-ray amorphous BN and Si<sub>3</sub>N<sub>4</sub> at 900 °C. During the deposition, reaction (9) and reaction (10) are simultaneous, forming the B-N and Si-N. Different SiCl<sub>4</sub> flow rates lead to different ratios of BN and Si<sub>3</sub>N<sub>4</sub>. As the SiCl<sub>4</sub> flow rate increases from 10 mL/min to 20 mL/min, reaction (10) is promoted whereas reaction (9) is influenced slightly, when NH<sub>3</sub> is in excess compared with SiCl<sub>4</sub> and BCl<sub>3</sub>.

As a consequence, the deposition rate largely improves. This results in the increase of Si element in the coating and thus in the observed increase of Si-N bonding. However, when the  $\text{SiCl}_4$  flow rate increases from 20 mL/min to 30 mL/min, reaction (10) is promoted greatly, and there is not enough  $\text{NH}_3$  to be consumed in reaction (9). As a result, the amount of B is reduced as shown by the reduction of the B-N bonding XPS peak. On the contrary, Si content increased as shown by the increase of the Si-N bonding XPS peak. At 900 °C, reaction (9) is still the main reaction. Because reaction (10) is promoted and (9) is restrained, the deposition rate is reduced at this range of the  $\text{SiCl}_4$  flow rate.

#### 4. Conclusions

The influence of the  $\text{SiCl}_4$  flow rate on the deposition rate, morphology, phase composition, chemical composition, and bonding states of SiBN coating deposited by low pressure chemical vapor deposition (LPCVD) at 900 °C has been investigated using  $\text{SiCl}_4\text{-BCl}_3\text{-NH}_3\text{-H}_2\text{-Ar}$  gas environment in this study. The deposition rate increases at first and then decreases with the increase of  $\text{SiCl}_4$  flow rate. The surface of the coating is a uniform cauliflower-like structure at 10 mL/min and 20 mL/min, and covered with small spherical particles at 30 mL/min. The coating deposited at various  $\text{SiCl}_4$  flow rates is X-ray amorphous, and contains Si, B, N, and O elements. The main bonding states are B-N, Si-N, and N-O. The amount of B element and B-N bonding decrease with the increase of  $\text{SiCl}_4$  flow rate, while Si element and Si-N bonding increase. The main deposition mechanism refers to two parallel reactions of  $\text{BCl}_3\text{+NH}_3$  and  $\text{SiCl}_4\text{+NH}_3$ . The deposition process is mainly controlled by the reaction of  $\text{BCl}_3\text{+NH}_3$ .

**Acknowledgments:** The authors acknowledge the support of the Chinese National Foundation for Natural Sciences under Contracts (No. 51472201, No. 51602258), the fundamental research funds for the central universities (No. 3102014KYJD011), the fund of State Key Laboratory of Solidification Processing in NWPU (No. SKLSP201401, No. KP201504), the Natural Science Foundation of Shaanxi Province (No. 2014JQ6197), the major national scientific instrument and equipment development project (2011YQ12007504), and Shaanxi International cooperation and exchange of scientific projects (No. 2015KW-015).

**Author Contributions:** Jianping Li and Yongsheng Liu conceived and designed the experiments; Jianping Li and Zan Li performed the experiments; Hailong Qin and Fang Ye analyzed the data; Laifei Cheng and Litong Zhang contributed reagents/materials/analysis tools; Jianping Li wrote the paper. The founding sponsors had no role in the design of the study; in the collection, analyses, or interpretation of data; in the writing of the manuscript, and in the decision to publish the results.

**Conflicts of Interest:** The authors declare no conflict of interest.

#### References

1. Naslain, R. Design, preparation and properties of non-oxide cmcs for application in engines and nuclear reactors: An overview. *Compos. Sci. Technol.* **2004**, *64*, 155–170. [[CrossRef](#)]
2. Rosso, M. Ceramic and metal matrix composites: Routes and properties. *J. Mater. Process. Technol.* **2006**, *175*, 364–375. [[CrossRef](#)]
3. Morscher, G.N. The effect of static and cyclic tensile stress and temperature on fatigue for precracked hi-nicalon/bn/cvd sic minicomposites in air. In Proceedings of the 21st Annual Conference on Composites, Advanced Ceramics, Materials, and Structures—A: Ceramic Engineering and Science Proceedings, Cocoa Beach, FL, USA, 12–16 January 1997; John Wiley & Sons, Inc.: Hoboken, NJ, USA, 2008; pp. 737–745.
4. Morscher, G.N. Tensile stress rupture of sicf/sicm minicomposites with carbon and boron nitride interphases at elevated temperatures in air. *J. Am. Ceram. Soc.* **1997**, *80*, 2029–2042. [[CrossRef](#)]
5. Dugne, O.; Prouhet, S.; Guette, A.; Naslain, R.; Fourmeaux, R.; Khin, Y.; Sevely, J.; Rocher, J.P.; Cotteret, J. Interface characterization by tem, aes and sims in tough SiC (ex-PCS) fibre-SiC (CVI) matrix composites with a bn interphase. *J. Mater. Sci.* **1993**, *28*, 3409–3422. [[CrossRef](#)]
6. Hurwitz, F.I.; Scott, J.M.; Chayka, P.V. Progress on bn and doped-bn coatings on woven fabrics. In Proceedings of the 25th Annual Conference on Composites, Advanced Ceramics, Materials, and Structures: A: Ceramic Engineering and Science Proceedings, Cocoa Beach, FL, USA, 21–27 January 2001; John Wiley & Sons, Inc.: Hoboken, NJ, USA, 2008; pp. 389–397.
7. Bryant, D.R. Oxidation and Volatilization of Bn Interphases in Sic Fiber-Reinforced Sic Matrix Composites. Master's Thesis, The Pennsylvania State University—University Park, State College, PA, USA, 1997.

8. Moore, A.W.; Sayir, H.; Fanner, S.C.; Morscher, G.N. Improved interface coatings for sic fibers in ceramic composites. In Proceedings of the 19th Annual Conference on Composites, Advanced Ceramics, Materials, and Structures-A: Ceramic Engineering and Science Proceedings, Cocoa Beach, FL, USA, 8–12 January 1995; John Wiley & Sons, Inc.: Hoboken, NJ, USA, 2008; pp. 409–416.
9. Nakamura, K.; Sasaki, T. Preparation of sibn films deposited by MOCVD. *J. Solid State Chem.* **2004**, *177*, 542–546. [[CrossRef](#)]
10. Essafti, A.; Go'mez-Aleixandre, C.; Albella, J.M. Preparation of SINB films by cvd techniques: Effect of  $\text{SiH}_4$  addition to  $\text{B}_2\text{H}_6$  and  $\text{NH}_3$  gas mixtures. *Diam. Relat. Mater.* **1996**, *5*, 580–583. [[CrossRef](#)]
11. Li, Z. Process and Structure of SIBN Interphase Manufactured by CVD/CVI. Master's Thesis, Northwestern Polytechnical University, Xi'an, China, 2014. (In Chinese)
12. Li, Z.; Cheng, L.; Liu, Y.; Ye, F. Thermodynamic analysis of chemical vapor deposition of  $\text{BCL}_3\text{-NH}_3\text{-SiCL}_4\text{-H}_2\text{-Ar}$  system. *J. Wuhan Univ. Technol.-Mater. Sci. Ed.* **2015**, *30*, 951–958. [[CrossRef](#)]
13. Liu, Y.; Chai, N.; Qin, H.; Li, Z.; Ye, F.; Cheng, L. Tensile fracture behavior and strength distribution of SiCf/SiC composites with different sibn interface thicknesses. *Ceram. Int.* **2015**, *41*, 1609–1616. [[CrossRef](#)]
14. Liu, Y.; Chai, N.; Li, Z.; Ye, F.; Liu, X.; Cheng, L. Effect of deposition temperature on deposition kinetics and mechanism of silicon boron nitride coating deposited from  $\text{BLC}_3\text{-NH}_3\text{-SiCL}_{14}\text{-H}_2\text{-Ar}$  mixture using low pressure chemical vapor deposition. *Surf. Coat. Technol.* **2015**, *261*, 295–303. [[CrossRef](#)]
15. Meng, G. *Chemical Vapor Deposition and New Inorganic Materials*; Science Press Ltd.: Beijing, China, 1984; pp. 78–79. (In Chinese)



© 2017 by the authors. Licensee MDPI, Basel, Switzerland. This article is an open access article distributed under the terms and conditions of the Creative Commons Attribution (CC BY) license (<http://creativecommons.org/licenses/by/4.0/>).